THROMBOSIS AND HEMOSTASIS

A CCR2 macrophage endocytic pathway mediates extravascular fibrin clearance in vivo

Michael P. Motley,[1,*] Daniel H. Madsen,[1-3,*] Henrik J. Jürgensen,[1,3] David E. Spencer,[1] Roman Szabo,[1] Kenn Holmbeck,[4] Matthew J. Flick,[5] Daniel A. Lawrence,[6] Francis J. Castellino,[7] Roberto Weigert,[1] and Thomas H. Bugge[1]

[1]Oral and Pharyngeal Cancer Branch, National Institute of Dental and Craniofacial Research, National Institutes of Health, Bethesda, MD; [2]Center for Cancer Immune Therapy, Department of Haematology, Herlev University Hospital, Herlev, Denmark; [3]Finsen Laboratory, Biotech Research and Innovation Center, Rigshospitalet, University of Copenhagen, Copenhagen, Denmark; [4]Craniofacial and Skeletal Diseases Branch, National Institute of Dental and Craniofacial Research, National Institutes of Health, Bethesda, MD; [5]Division of Experimental Hematology and Cancer Biology, Cincinnati Children's Hospital, Cincinnati, OH; [6]Division of Cardiovascular Medicine, Internal Medicine, University of Michigan Medical School, Ann Arbor, MI; and [7]W. M. Keck Center for Transgene Research and Department of Chemistry and Biochemistry, University of Notre Dame, Notre Dame, IN

Key Points

- Fibrin is cleared from extravascular space via endocytosis and lysosomal degradation by a CCR2-positive subset of inflammatory macrophages.
- This novel endocytic fibrin degradation pathway is mechanistically coupled to extracellular fibrin degradation pathways.

Extravascular fibrin deposition accompanies many human diseases and causes chronic inflammation and organ damage, unless removed in a timely manner. Here, we used intravital microscopy to investigate how fibrin is removed from extravascular space. Fibrin placed into the dermis of mice underwent cellular endocytosis and lysosomal targeting, revealing a novel intracellular pathway for extravascular fibrin degradation. A C-C chemokine receptor type 2 (CCR2)-positive macrophage subpopulation constituted the majority of fibrin-uptaking cells. Consequently, cellular fibrin uptake was diminished by elimination of CCR2-expressing cells. The CCR2-positive macrophage subtype was different from collagen-internalizing M2-like macrophages. Cellular fibrin uptake was strictly dependent on plasminogen and plasminogen activator. Surprisingly, however, fibrin endocytosis was unimpeded by the absence of the fibrin(ogen) receptors, αMβ2 and ICAM-1, the myeloid cell integrin-binding site on fibrin or the endocytic collagen receptor, the mannose receptor. The study identifies a novel fibrin endocytic pathway engaged in extravascular fibrin clearance and shows that interstitial fibrin and collagen are cleared by different subsets of macrophages employing distinct molecular pathways. (*Blood*. 2016;127(9):1085-1096)

Introduction

Conversion of fibrinogen into the insoluble polymer, fibrin, stems blood loss after vessel rupture. Furthermore, fibrin deposited in extravascular space forms a provisional matrix that supports cell migration during tissue repair and is critical for controlling initial stages of bacterial infection.[1-5]

Because of its potent proinflammatory properties, the rate of deposition and removal of extravascular fibrin must be carefully coordinated. This is illustrated by the inflammation-associated multiorgan pathology and impaired tissue regenerative capacity of humans and mice deficient in the key fibrinolytic protease zymogen, plasminogen,[6-17] as well as by the capacity of extravascular fibrin to exacerbate the morbidity of a range of chronic human diseases, including multiple sclerosis, tissue fibrosis, muscular dystrophy, and rheumatoid arthritis.[18-24]

Plasminogen is a serine protease zymogen present in plasma and extravascular fluids that is converted to the active protease plasmin by endoproteolytic cleavage by the closely related trypsin-like serine proteases urokinase plasminogen activator (uPA) and tissue plasminogen activator (tPA).[25,26]

Four pathways for plasminogen activation are known in the context of physiological fibrinolysis: (1) fibrin-dependent tPA-mediated plasminogen activation, in which fibrin binds plasminogen and tPA to bring the two molecules in close apposition to favor plasminogen activation[27-30]; (2) cell-dependent, tPA-mediated plasminogen activation, which involves the receptor-mediated binding of tPA and plasminogen to the cell surface[31-38]; (3) cell-dependent, uPA-mediated plasminogen activation, which involves the binding of uPA to the uPA receptor (uPAR) and receptor-mediated binding of plasminogen to the cell surface[39-44]; and (4) a poorly understood uPAR-independent, uPA-mediated plasminogen activation pathway, which may be cell dependent or cell independent.[15,17,45-54] Although mechanistically distinct, these pathways display considerable functional redundancy in extravascular fibrin surveillance.[15,17,45-53]

The enzymatic pathways that facilitate productive plasmin formation are well defined, but the cellular and molecular mechanisms by which fibrin ultimately is cleared from extravascular space are poorly investigated. Plasmin digestion of fibrin ex vivo results in the release of fibrin degradation products of high molecular weight.[55] Extravascular

Submitted May 11, 2015; accepted November 30, 2015. Prepublished online as *Blood* First Edition paper, December 8, 2015; DOI 10.1182/blood-2015-05-644260.

*M.P.M. and D.H.M. contributed equally to this study.

The online version of this article contains a data supplement.

There is an Inside *Blood* Commentary on this article in this issue.

The publication costs of this article were defrayed in part by page charge payment. Therefore, and solely to indicate this fact, this article is hereby marked "advertisement" in accordance with 18 USC section 1734.

fibrin deposits are infiltrated by leukocytes,[15,39,51,53,56] and cultured primary macrophages, human peripheral blood mononuclear cells, and monocytoid cell lines all can endocytose soluble fibrin monomer.[57,58] Furthermore, early electron microscopy studies reported an abundance of fibrillar material morphologically consistent with fibrin in leukocytes associated with extravascular fibrin deposits in rheumatoid arthritis.[59-61] This suggests that extravascular fibrin degradation may be orchestrated at the cellular level and include an intracellular lysosomal step.

To gain insight into the process of extravascular fibrin degradation, we used intravital imaging with subcellular resolution to directly visualize the dissolution of fibrin matrices placed within subcutaneous space and to identify the cell types, enzymes, and receptors involved. We report that fibrin is degraded predominantly by a C-C chemokine receptor type 2 (CCR2)-positive subpopulation of macrophages via a plasmin-dependent endocytic mechanism that is functional in the absence of the established fibrin(ogen) receptors αMβ2 (Mac-1, CD11b/CD18) and intercellular adhesion molecule 1 (ICAM-1) or the integrity of the major integrin-binding site on fibrin.

Materials and methods

Mice

Animal procedures were performed in an Association for Assessment and Accreditation of Laboratory Animal Care–accredited vivarium under approved protocols. Mouse strain and genotyping details are in supplemental Table 1 (available on the *Blood* Web site).

Isolation of fibrinogen from mouse plasma

Citrated plasma in Tris-buffered saline, 5 mM benzamidine, and 200 U/mL aprotinin was precipitated twice with 25% saturated $(NH_4)_2SO_4$ at room temperature for 15 min. The precipitate was resuspended in 50 mM imidazole and 100 mM NaCl, dialyzed against HEPES-buffered saline, and stored at −80°C. Fibrinogen (1 mg) was fluorescently conjugated using the Alexa Fluor 488 protein-labeling kit (Life Technologies) as per the manufacturer's recommendations.

Fluorescent fibrin gel formation

Fluorescent fibrin gels were made by polymerizing plasminogen-depleted, FXIII-containing fibrinogen with thrombin in the presence of Alexa-conjugated human fibrinogen. The detailed procedure is found in supplemental Data.

Implantation of fibrin gel and tissue imaging

A 1-cm dorsal incision was made on the left side of the spine of isoflurane-anesthetized mice. Labeled fibrin gel was placed into a subcutaneous pocket made under the left flank. The pocket was filled with a 250-μL solution of 0.4 mg/mL Alexa Fluor 647 (10 000 MW), anionic, fixable dextran or Texas red (10 000 MW), lysine fixable dextran (Life Technologies) in phosphate-buffered saline (PBS), and the incision was closed with wound clips. Mice were administered Hoechst 33342 intravenously as previously described[62] and killed by CO_2 inhalation 3 to 4 hours later. Immediately thereafter, the location of the fibrin gel was determined with a NightSea DFP-1 Dual Fluorescent Protein Flashlight, and the dermis over the detected gel was marked and excised with a 10-mm margin around the edge. The tissue was immediately imaged by confocal microscopy or whole-mount immunostained. Confocal imaging was performed using an inverted confocal microscope (IX81; Olympus) equipped with a scanning head (FluoView 1000; Olympus) as described previously.[62] Details on imaging are found in supplemental Data.

Quantitative analysis of cellular fibrin uptake

Three to five 30-μm z-stacks were collected from each sample, first identifying with the EPI scope the point of highest fibrin signal and acquiring stacks 1500 μm above, left, below, and right of this point. Cell number in each z-stack was determined by counting all nuclei stained with Hoechst dye. Internalization was scored as the presence of fluorescently labeled fibrin in vesicular structures around Hoechst-labeled nuclei. The percentage of cells positive for internalization or the percentage of CCR2-RFP–, Cx3Cr1-GFP-, or Col1a1-GFP–positive cells was calculated by dividing the number of cells scored positive for that signal by the total number of cells. Imaris 3D reconstruction software (Bitplane, South Windsor, CT) was used for image generation.

Whole-mount tissue staining

Whole-mount staining of tissues was performed as described previously.[62] Details on antibodies and incubation conditions are found in supplemental Data.

Quantitative fibrin degradation assay

Alexa Fluor 488–labeled fibrin gels were implanted subcutaneously as described above. For each time point, at least 3 control gels in PBS containing 0.5% sodium azide were left in the dark at 37°C as reference. Mice were killed, and fibrin gels were visualized and removed using the NightSea flashlight. The gels were weighed and dissolved overnight at 37°C in 1.5 mL 5 mg/mL trypsin, 4.8 mM EDTA. Vortexed samples were centrifuged at 16 000*g* for 2 minutes, dispensed in 100-μL aliquots into Costar 96-well black clear-bottom plates, and read with a Synergy Neo HTS multimode microplate reader (BioTek) with the absorption wavelength at 488 nm and emission wavelength at 520 nm. Alexa Fluor 488–conjugated fibrinogen in PBS was used to produce standard curves.

Flow cytometry

Flow cytometry was performed using cells isolated from fibrin implantation zones. Details on analysis are found in supplemental Data.

Real-time PCR

Real-time PCR analysis was done on cells isolated by fluorescence-activated cell sorting using TaqMan gene expression arrays. Details on analysis are found in supplemental Data.

Diphtheria toxin depletion of CCR2-expressing cells

CCR2-depleter$^{+/0}$ and littermate control mice were implanted with fibrin gels. The mice received daily intraperitoneal injections with 50 ng/g body weight diphtheria toxin, starting 1 day prior to gel implantation and continuing until termination at 24 hours after fibrin implantation.

Results

An assay to image endocytic fibrin degradation in vivo

To explore if the degradation of extravascular fibrin involves endocytic uptake, we developed an assay to directly visualize the fate of fibrin gels placed in extravascular space. We generated fibrin gels ex vivo by polymerizing fibrinogen with thrombin. The gels incorporated fibrinogen labeled with Alexa Fluor 488, 594, or 647, which are pH insensitive, photostable fluorescent dyes that can be visualized in various extracellular and intracellular compartments during in vivo imaging procedures[62,63] (see "Materials and methods" for details on this and other procedures). In agreement with the reported photostability, fibrin gels stored in the dark at 37°C in PBS with sodium azide lost just 8% fluorescence signal in 14 days, when compared with control gels stored in the dark

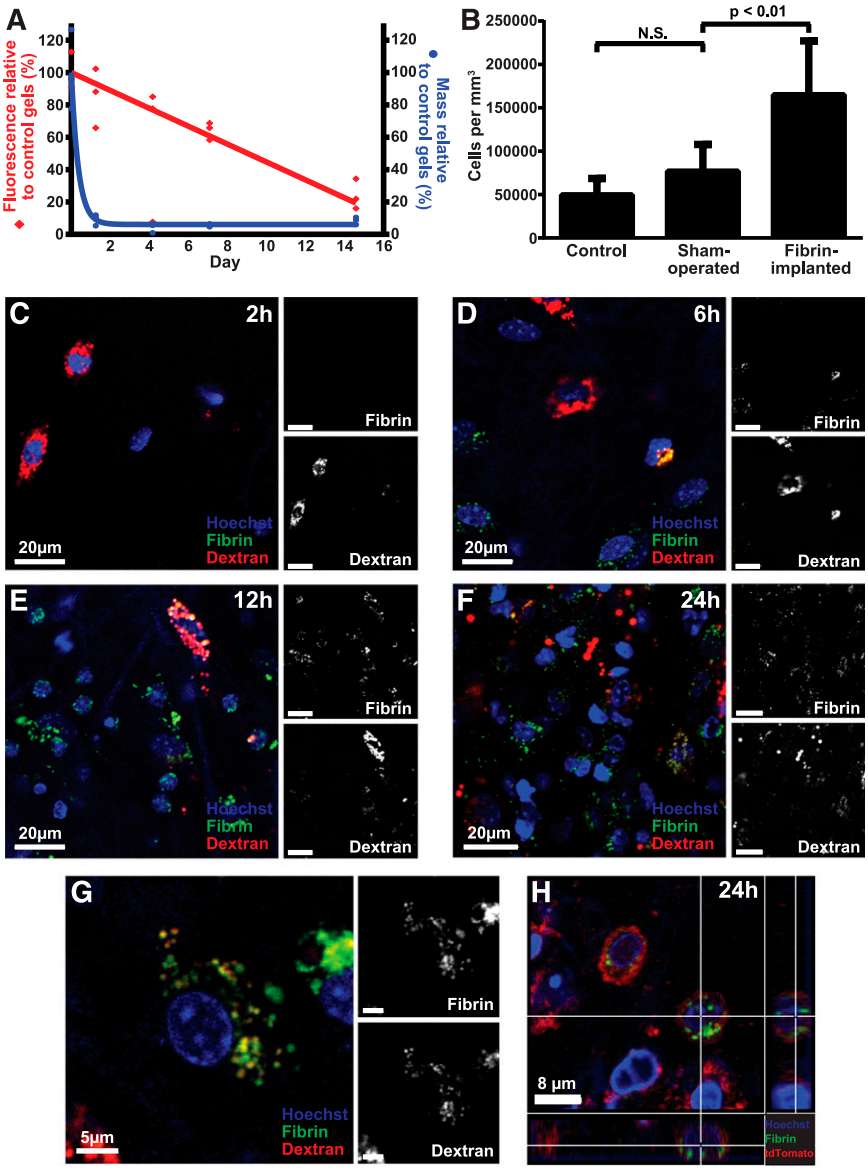

Figure 1. Endocytic degradation of extravascular fibrin in vivo. (A) Fluorescent fibrin gels placed in subcutaneous space undergo degradation. Alexa Fluor 488–labeled fibrin gels were placed in the dermis of mice. The gels were extracted at the indicated time points, and gel weight (blue circles) and total fluorescence (red diamonds) were determined. Data are expressed as percent residual weight and residual fluorescence, as compared with control gels stored for the identical time period in the dark at 37°C in PBS with sodium azide. Triplicate readings for each sample were made and divided by the mean reading of the control gels to yield percent remaining fluorescence. (B) Fibrin implantation causes cell recruitment. Total cell number in control (left bar), sham-operated (middle bar), and fibrin-implanted (right bar) mice at 24 hours, as determined by the counting of nuclei in serial z-stacks from the implantation zone. Data are shown as mean ± standard deviation. N = 7 mice for control, 7 for sham operated, and 12 for fibrin-implanted mice. Significance was determined by 1-way ANOVA. (C-G) Fibrin implanted to subcutaneous space undergoes cellular endocytosis. (C-F) Representative images of mouse dermis 2, 6, 12, and 24 hours postinjection show progressive accumulation of cells that present with fluorescently labeled fibrin (green, white in top insets) in perinuclear vesicles sometimes colocalizing with the Alexa Fluor 647 dextran lysosomal marker (red, white in bottom insets). (G) High magnification of a single fibrin-internalizing cell showing the colocalization of fibrin (green, white in top inset) and dextran (red, white in bottom inset) in perinuclear vesicles (yellow), indicative of lysosomal routing of endocytosed fibrin. (H) Fibrin uptake (green) by cells 24 hours after fibrin implantation in *Gt(ROSA)26Sortm4 (ACTB-tdTomato,-EGFP)Luo*$^{+/0}$ transgenic mice expressing plasma membrane–localized tomato fluorescent protein (red). Cross hairs mark a cell with multiple fibrin-containing vesicles completely circumscribed by plasma membrane. N.S., not significant.

at −80°C. We first implanted fluorescent fibrin gels into the subcutis of mice to determine the fate of fibrin placed in extravascular space. Mice were killed 1.25, 4, 7, and 15 days later, the gels were extracted, and their weight and total fluorescence was compared with control gels stored in the dark at 37°C in PBS with sodium azide for the identical time period (Figure 1A). The weight of the implanted fibrin gels decreased rapidly to 9% of their original weight within 30 hours. In contrast, the fluorescence of implanted gels displayed a slower reduction with time, with a half-life of ~9 days.

To determine the cellular contribution to extravascular fibrin degradation in vivo, we implanted fluorescently labeled fibrin together with Alexa Fluor 647–labeled 10 kDa dextran, which accumulates in lysosomes within 2 hours of administration.[62,64,65] Furthermore, we systemically injected fluorescent Hoechst 33342 dye prior to imaging to visualize cell nuclei.[62] Enumeration of cell density in the fibrin implantation zone, by analysis of confocal z-stacks, revealed a large increase in cellularity, when compared with control mice or mice undergoing sham surgery, showing that fibrin implantation causes cell recruitment (Figure 1B). Inspection of confocal z-stacks 2, 6, 12, and 24 hours after fibrin implantation showed progressive accumulation of cells within the fibrin implantation zone (Figure 1C-F). Importantly, most cells within the implantation zone displayed fibrin-containing intracellular vesicles. Many of these fibrin-containing vesicles colocalized with the Alexa Fluor 647 dextran lysosomal marker (Figure 1G), suggesting that endocytosed extravascular fibrin is targeted to the lysosome. To provide independent support for an endocytic pathway for extravascular fibrin clearance, we implanted fluorescent fibrin into mice that express plasma membrane-localized tdTomato fluorescent protein.[66] Inspection of confocal z-stacks from fibrin implantation zones of these mice indeed revealed numerous fibrin-containing vesicles completely circumscribed by plasma membrane (Figure 1H). Taken together, these data show that degradation of extravascular fibrin involves endocytosis and lysosomal targeting.

CCR2-positive macrophages accumulate in response to extravascular fibrin deposition and constitute the dominant cell population engaged in endocytic fibrin degradation

We set out to identify the cell types engaged in endocytic degradation of extravascular fibrin. For this purpose, we used a combination of

whole-mount staining with antibodies against cell-type–specific markers and transgenic mice expressing cell-type–specific fluorescent tags. Interestingly, 54.7% of all cells observed within the fibrin implantation zone at 24 hours postimplantation expressed the pan-macrophage marker F4/80. Furthermore, 58.3% of these cells endocytosed fibrin, and 70.2% of all fibrin-endocytosing cells were F4/80 positive, suggesting a key role of macrophages in mediating extravascular fibrin internalization (Figure 2A,B,G,H). In contrast, whole-mount staining using the neutrophil marker NIMP.R14 revealed that neutrophils constituted only 11.4% of cells in the fibrin implantation zone and just 4.9% of fibrin-uptaking cells, suggesting a minor contribution of neutrophils to endocytic fibrin degradation (Figure 2C,D,G,H). To determine if nonleukocyte cell populations contribute to endocytic fibrin turnover, we implanted fibrin gels into mice hemizygous for a *Col1a1*-GFP transgene (*Col1a1-GFP*$^{+/0}$ mice) expressed in dermal fibroblasts[67] and quantified the abundance of GFP-positive cells in the implantation zone and their uptake of fibrin. This revealed that dermal fibroblasts engage in extravascular fibrin turnover to a minor extent, constituting 6.4% of all cells and 9.7% of all fibrin-uptaking cells (Figure 2E-H). A total of 27.5% of all cells (Figure 2G) and 15.3% of fibrin-internalizing cells (Figure 2H) in fibrin implantation zones did not score as macrophages, neutrophils, or fibroblasts, as defined by expression of either of the 3 markers. These cells may be macrophages, neutrophils, or fibroblasts expressing insufficient levels of, respectively, F4/80, NIMP.R14, or the Col1a1-GFP transgene to be scored as positive or may represent an unidentified cell population. This analysis reveals a dominant role of macrophages in endocytic fibrin uptake, with minor contributions from neutrophils and fibroblasts.

Tissue-infiltrating macrophages arise from distinct populations of circulating CCR2-positive, CX3CR1-negative (or CCR2-positive, CX3CR1-low expressing) and CCR2-negative, CX3CR1-positive monocytes.[68] To determine if specific subpopulations of macrophages engaged in endocytic fibrin degradation, we implanted fibrin into mice that carried 1 wild-type and 1 RFP-tagged *Ccr2* allele (*CCR2*$^{+/RFP}$ mice) and quantified cellular fibrin uptake after 24 hours. CCR2-positive macrophages constituted 38.6% of all cells and 54.4% of all fibrin-uptaking cells within the implantation zone (Figure 3A-B). Quantification of cellular fibrin uptake after implantation of fluorescent fibrin gels into mice that carry 1 wild-type and 1 GFP-tagged *Cx3cr1* allele (*Cx3cr1*$^{+/GFP}$ mice) showed that CX3CR1-positive macrophages constituted 32.2% of all cells and 40.9% of all fibrin-uptaking cells (Figure 3D-E). We next implanted fibrin into mice that carried 1 wild-type and 1 GFP-tagged *Cx3cr1* allele as well as 1 RFP-tagged *Ccr2* allele (*Cx3cr1*$^{+/GFP}$; *CCR2*$^{+/RFP}$ mice). Interestingly, nearly all CX3CR1-positive cells and nearly all fibrin-endocytosing CX3CR1-positive cells were also positive for CCR2, with CX3CR1 single-positive cells constituting just 1.36% of all cells and 1.40% of all fibrin-uptaking cells (Figure 3G-H). These macrophage populations, in part, accumulated in response to fibrin implantation, with the density of CCR2-positive cells in fibrin-implanted mice being, respectively, 25.4- and 5.4-fold higher than control and sham-operated mice, and the density of CX3CR1-positive cells being, respectively, 34.5- and 1.75-fold higher than control and sham-operated mice (Figure 3C,F).

Fibrin-uptaking cells were morphologically different from collagen-degrading macrophages[62] by being smaller with fewer and smaller lysosomes. This indicated that fibrin- and collagen-endocytosing macrophages constitute distinct macrophage subpopulations. Consistent with this, analysis of injection fields from fibrillar collagen-injected

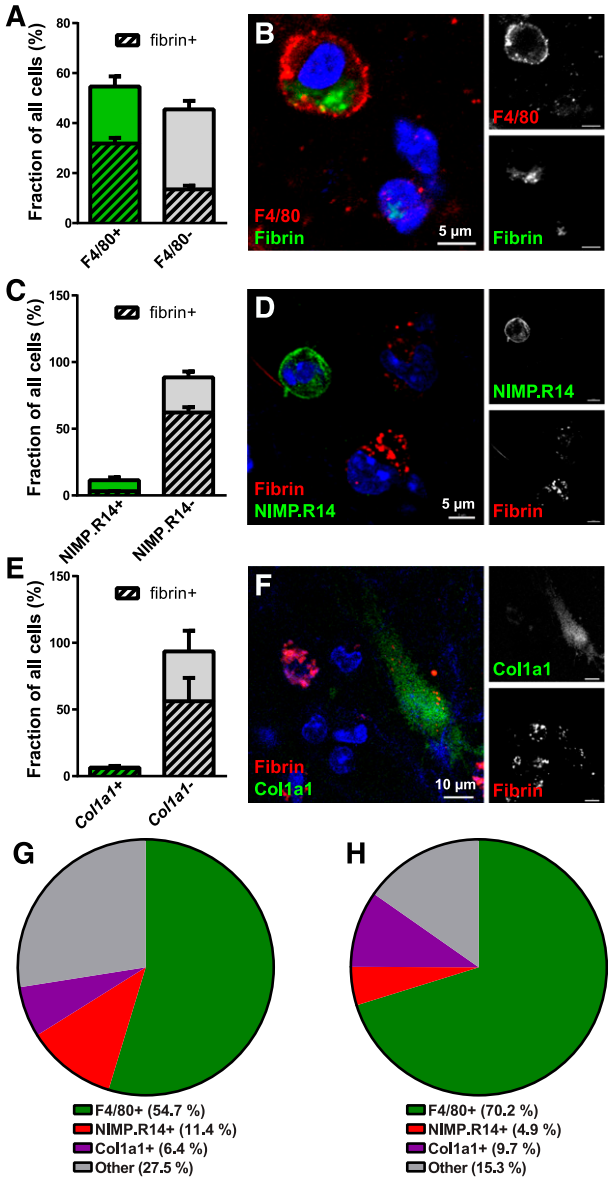

Figure 2. Macrophages are the principal cells mediating extravascular fibrin endocytosis in vivo. (A-B) Endocytic fibrin uptake by F4/80-positive cells. (A) Percentage F4/80-positive (green bar) and F4/80-negative (gray bar) cells in fibrin implantation zones. Crosshatched bars embedded within green and gray bars show fraction of, respectively, F4/80-positive and F4/80-negative cells that endocytose fibrin. Whole-mount immunostaining was performed 24 hours after fibrin implantation. Data were generated from serial analysis of confocal z-stacks from 3 mice as described in "Materials and methods." Error bars indicate standard deviation. (B) Example of a F4/80-positive (red, white in top right panel) fibrin-internalizing (green, white in bottom left panel) cell. (C-D) Endocytic fibrin-uptake by NIMP.R14-positive cells. (C) Percentage of NIMP.R14-positive (green bar) and NIMP.R14-negative (gray bar) cells in fibrin implantation zones. Crosshatched bars embedded in green and gray bars show fraction of, respectively, NIMP.R14-positive and NIMP.R14-negative cells that endocytose fibrin. Whole-mount immunostaining was performed 24 hours after subcutaneous fibrin implantation. Data were generated as in panel A from 3 mice. (D) Example of a NIMP.R14-positive (green, white in top right panel), fibrin-negative cell, and examples of NIMP.R14-negative fibrin-positive (red, white in top panel) cells. (E-F) Endocytic fibrin-uptake by Col1a1-GFP–positive cells. Percentage of GFP-positive (green bar) and GFP-negative (gray bar) cells in implantation zones from fibrin-implanted *Col1a1-GFP*$^{+/0}$ transgenic mice. Crosshatched bars embedded in green and gray bars show fraction of, respectively, GFP-positive and GFP-negative cells that endocytose fibrin. Data were generated as in panel A from 3 mice. (F) Example of an GFP-positive (green, white in top right panel) fibrin-internalizing (red, white in bottom left panel) cell. (G-H) Pie charts showing the constitution of all cells (G) and fibrin-internalizing cells (H) in the fibrin implantation zone.

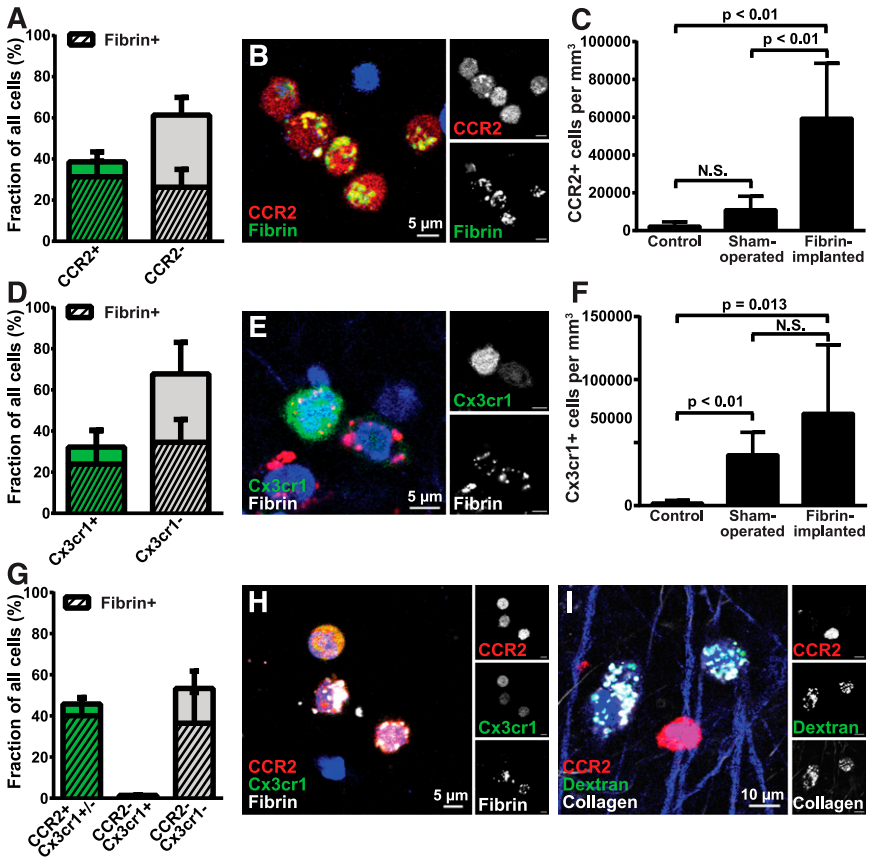

Figure 3. CCR2-positive and CCR2-CX3CR1 double-positive macrophages accumulate in fibrin deposits and mediate endocytic fibrin uptake. (A) Endocytic fibrin uptake by CCR2-positive cells. Percentage CCR2-positive (green bar) and CCR2-negative (gray bar) cells 24 hours after implantation of fibrin into *CCR2*$^{+/RFP}$ transgenic mice. Crosshatched bars embedded within green and gray bars show fraction of, respectively, CCR2-positive and CCR2-negative cells that endocytose fibrin. Data were generated from serial analysis of confocal z-stacks from 5 mice as described in "Materials and methods." Error bars indicate standard deviation. (B) Examples of CCR2-positive (red, white in top right panel) cells with endocytosed fibrin 24 hours after fibrin implantation. (C) CCR2-positive cells accumulate in fibrin implantation zones. Total number of CCR2-positive cells in control (left bar), sham-operated (middle bar), or fibrin-implanted (right bar) dermis at 24 hours, as determined by the counting of cells in 4 serial z-stacks from the implantation zone. Data are shown as mean ± standard deviation and were generated by analysis of 4 control, 4 sham-operated, and 5 fibrin-implanted mice. Significance was determined by 1-way ANOVA. (D) Endocytic fibrin uptake by CX3CR1-positive cells. Percentage CX3CR1-positive (green bar) and CX3CR1-negative (gray bar) cells 24 hours after implantation of fibrin into *Cx3cr1*$^{+/GFP}$ transgenic mice. Crosshatched bars embedded within green and gray bars show fraction of, respectively, CX3CR1-positive and CX3CR1-negative cells that endocytose fibrin. Data were generated from serial analysis of confocal z-stacks from 5 mice as described in "Materials and methods." Error bars indicate standard deviation. (E) Examples of a CX3CR1-positive cell (green, white in top right panel) with endocytosed fibrin (red, white in bottom right corner) 24 hours after fibrin implantation. (F) CX3CR1-positive cells accumulate in fibrin implantation zones. Total number of CX3CR1-positive cells in control (left bar), sham-operated (middle bar), or fibrin-implanted (right bar) dermis at 24 hours, as determined by the counting of cells in 4 serial z-stacks from the implantation zone. Data are shown as mean ± standard deviation and were generated by analysis of 5 control, 8 sham-operated, and 10 fibrin implanted mice. Significance was determined by 1-way ANOVA. (G) CCR2 single-positive and CCR2, CX3CR1 double-positive cells constitute the majority of fibrin-uptaking cells. Percentage of CCR2 single-positive and CCR2, CX3CR1 double-positive (left bar) and CX3CR1-negative (middle bar), and CCR2, CX3CR1 double-negative cells 24 hours after implantation of fibrin into *Cx3cr1*$^{+/GFP}$;*CCR2*$^{+/RFP}$ bitransgenic mice. Crosshatched bars embedded in bars show fraction of, respectively, CCR2-positive and CCR2-negative cells that endocytose fibrin. A total of 32% of the cells in the left bar are CCR2 single positive and 68% are CCR2, CX3CR1 double positive. Data were generated from serial analysis of confocal z-stacks from 4 mice as described in "Materials and methods." Error bars indicate standard deviation. (H) Examples of CCR2, CX3CR1 double-positive cells (orange/yellow, white top right and middle panels) with endocytosed fibrin (white) 24 hours after fibrin implantation. (I) CCR2-positive cells do not engage in endocytic collagen degradation. Representative example of injection field from *Cx3cr1*$^{+/GFP}$;*CCR2*$^{+/RFP}$ bitransgenic mice 24 hours after injection with fluorescently labeled fibrillar collagen. Collagen-uptaking (white) CCR2-negative cells and a collagen-negative, CCR2-positive (red, white top right corner) cell are shown.

CCR2$^{+/RFP}$ mice showed that collagen endocytosing cells and CCR2-positive cells were distinct cell populations (Figure 3I).

Fibrin-internalizing cells have low proliferation rate and express plasminogen activator

We next isolated CD45-positive cells from fibrin implantation zones and performed flow cytometry analysis after staining with antibodies against the proliferation marker Ki-67. This analysis showed that fibrin-internalizing and fibrin noninternalizing CD45-positive cells displayed low proliferation rates (Figure 4A-E). Of potential interest, a 4.5-fold reduction in Ki-67–positive cells was observed in fibrin-internalizing cells compared with noninternalizing cells, tentatively suggesting that fibrin uptake may modulate cell proliferation. However, CCR2 fibrin-positive and fibrin-negative cells could not be compared directly, due to loss of RFP signal by cell permeabilization.

To analyze the expression of plasminogen activator, we performed real-time PCR of populations of CD45, CCR2 double-positive fibrin-internalizing and CD45-positive fibrin-noninternalizing cells from fibrin implantation zones isolated by fluorescence-activated cell sorting (CD45, CCR2 double-positive cells were not obtained in sufficient numbers for analysis). Both fibrin-internalizing and fibrin-noninternalizing cells expressed uPA and uPAR messenger RNA (mRNA) at comparable levels (Figure 4F). tPA mRNA expression was below the detection limit (data not shown).

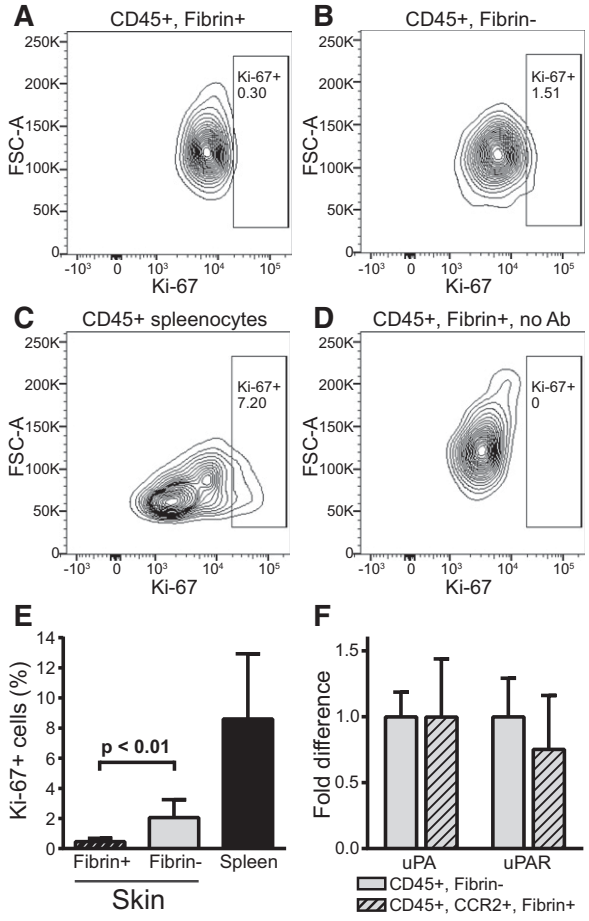

Figure 4. Fibrin-internalizing cells display a low proliferation rate and express components of the plasminogen activation system. (A-E) Analysis of proliferation of fibrin-uptaking and fibrin-nonuptaking cells from fibrin implantation zones. (A-B) Representative examples of flow cytometry analysis of CD45-positive, fibrin-internalizing cells (A) and CD45-positive, fibrin-noninternalizing cells (B) stained with Ki-67 antibodies. (C) Flow cytometry of CD45-positive spleen cells (positive control). (D) Flow cytometry analysis of CD45-positive, fibrin-internalizing cells with primary antibody omitted (negative control). Diagrams show intensity of Ki-67 staining vs forward scatter. Boxes show gate for positive signal, and percent of cells in gate is indicated. (E) Enumeration of Ki-67–positive, CD45-positive fibrin-uptaking (left bar, N = 6) and CD45-positive, fibrin-negative (middle bar, N = 6) cells. Ki-67 staining of CD45-positive spleen cells (N = 4) are shown in the right bar. Data are shown as mean with standard deviation. *P* value was determined by Student *t* test (2 tailed). (F) Real-time PCR analysis of *Plau* (left bars) and *Plaur* (right bars) mRNA expression in fluorescence-activated cell sorting–isolated CD45-positive, fibrin-negative (open bars) and CD45-positive, CCR2-positive, fibrin-positive (cross-hatched bars). Data are shown as mean with standard deviation and were generated from 3 samples, each sample being a pool of cells isolated from 3 mice. Ab, antibody; FSC-A, forward scatter-A.

Depletion of CCR2-positive cells reduces fibrin endocytosis

To determine the effect of the selective depletion of CCR2 macrophages on endocytic fibrin uptake, we used a transgenic mouse strain expressing the human diphtheria toxin receptor controlled by the *Ccr2* gene promoter (*CCR2-depleter*$^{+/0}$ mice[69]). This mouse was crossed to *CCR2*$^{+/RFP}$ mice to generate *CCR2*$^{+/RFP}$;*CCR2-depleter*$^{+/0}$ bitransgenic mice and *CCR2*$^{+/RFP}$ littermates. These mice were pretreated with diphtheria toxin and implanted with fibrin, and the fibrin implantation zones were analyzed 24 hours later. As expected, a dramatic reduction of CCR2-positive cells was observed in diphtheria toxin–treated *CCR2*$^{+/RFP}$;*CCR2-depleter*$^{+/0}$ bitransgenic mice, when compared with diphtheria toxin–treated single-transgenic *CCR2*$^{+/RFP}$ littermates (Figure 5A, examples in Figure 5C-D) and caused a 43% reduction in the total number of fibrin-endocytosing cells (Figure 5B). Fibrin uptake in CCR2-negative cells, characterized in Figure 3, was not affected by loss of CCR2-positive cells. The discrepancy in the abundance of these cells (Figure 3A and Figure 5B) may represent experimental variation and/or difference in method of quantitation (fraction of cells vs cells per volume unit).

Involvement of fibrin receptors and myeloid cell–fibrin recognition motifs in endocytic fibrin uptake in vivo

Myeloid cells bind purified fibrin via an interaction between the αMβ2 (Mac-1, CD11b/CD18) integrin and an integrin-binding RLTIGE (human)/RLSIGE (mouse) motif within the fibrinogen γ chain.[3,70,71] Furthermore, soluble fibrin monomer is endocytosed by cultured myeloid cells in an αMβ2-dependent manner.[58] Indeed, flow cytometry analysis showed that nearly all CCR2-positive, fibrin-internalizing cells expressed αMβ2 (Figure 6A-D), making αMβ2 a strong fibrin endocytosis candidate receptor. To determine if αMβ2 integrin is critical for endocytic fibrin uptake, we implanted fibrin into αM-deficient (*Itgam*$^{-/-}$) mice and wild-type littermates. Loss of αMβ2 caused a small, nonsignificant, increase of cells in the fibrin implantation zone (Figure 6M). Unexpectedly, however, loss of αMβ2 integrin did not affect endocytic fibrin uptake, as assessed by the fraction of cells with endocytosed fibrin, indicating that fibrin endocytosis can take place in the absence of this integrin (Figure 6Q). One possible explanation for this unanticipated result was that other β2 integrins engaged the RLSIGE fibrinogen γ-chain motif during fibrin endocytosis. To investigate this, we employed fibrinogen from *Fgg*$^{390\text{-}396A}$ knockin mice, in which the fibrinogen RLSIGE γ-chain motif is replaced by alanines. This mutant fibrinogen fails to support myeloid cell adhesion in vitro.[3] Fibrinogen was purified from *Fgg*$^{390\text{-}396A}$ mice and wild-type littermates, fluorescently labeled, and implanted into mice. Total cell numbers in fibrin implantation zones were similar in wild-type and mutant fibrin-implanted mice (Figure 6N). Surprisingly, analysis of implantation fields 24 hours after fibrin implantation showed no difference in the fraction of cells endocytosing mutant and wild-type fibrin (Figure 6R). The lack of evidence for involvement of a β2 integrin–dependent mechanism of cellular uptake led us to examine the contribution of ICAM-1, a non–integrin-type fibrin(ogen) receptor expressed on leukocytes.[72] Indeed, most fibrin-internalizing CCR2-positive cells expressed ICAM-1 (Figure 6E-H), and total cell accumulation in fibrin implantation zones was unaffected by ICAM-1 deficiency (Figure 6O). Thus, we implanted fibrin gels into ICAM-1–deficient (*Icam1*$^{-/-}$) mice and wild-type littermates and determined the fraction of cells internalizing fibrin after 24 hours (Figure 6S). Again, no effect of ICAM-1 deficiency was observed on fibrin endocytosis.

Mannose receptor (MR) is an endocytosis receptor responsible for macrophage-mediated collagen endocytosis,[62,73-76] and we found it to be is expressed in a subset of CCR2-positive fibrin-internalizing cells (Figure 6I-L). To examine if the mannose receptor functions as a fibrin endocytosis receptor, for example via a carbohydrate-mediated interaction, we implanted fibrin into MR-deficient (*Mrc1*$^{-/-}$) mice and wild-type littermates and analyzed cell accumulation (Figure 6P) and fibrin endocytosis (Figure 6T). This analysis revealed no effect of loss of mannose receptor on fibrin endocytosis. Overall, this analysis shows that fibrin endocytosis can take place in mice with individual deficiencies in αMβ2, ICAM-1, and MR.

Plasminogen and plasminogen activation are critical for endocytic fibrin uptake

We next investigated the involvement of extracellular proteases in endocytic fibrin uptake and, thus, the possible mechanistic coupling of extracellular and intracellular fibrin degradation pathways. Plasmin is

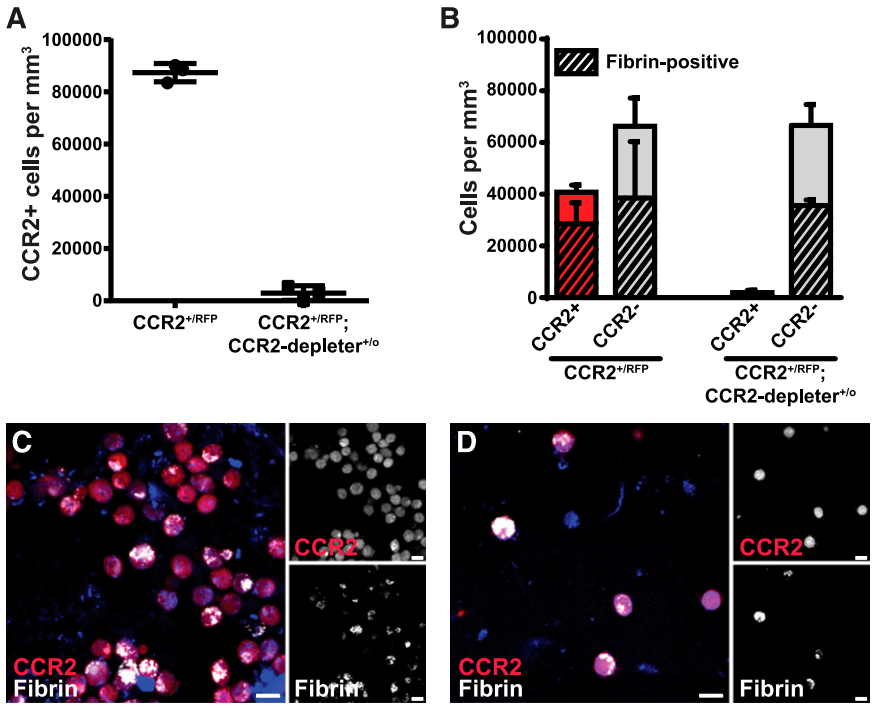

Figure 5. Depletion of CCR2-positive cells reduces endocytic fibrin uptake. *CCR2*$^{+/RFP}$ single-transgenic mice (N = 3) and *CCR2*$^{+/RFP}$;*CCR2-depleter*$^{+/0}$ bitransgenic littermates (N = 3), expressing the diphtheria toxin receptor selectively in CCR2-positive cells, were treated with diphtheria toxin and implanted with fluorescent fibrin. (A) Enumeration of CCR2-positive cells in fibrin implantation fields 24 hours after fibrin implantation. (B) Number of CCR2-positive (red bars) and CCR2-negative (gray bars, N = 3) cells 24 hours after implantation of fibrin into diphtheria toxin–treated *CCR2*$^{+/RFP}$ transgenic mice (left bars) and *CCR2*$^{+/RFP}$;*CCR2-depleter*$^{+/0}$ bitransgenic littermates (right bars, N = 3). Crosshatched bars embedded within red and gray bars show fraction of, respectively, CCR2-positive and CCR2-negative cells that endocytose fibrin. Data in panel A are shown as individual data points and as mean values with standard deviations. Significance was determined by Student *t* test (2 tailed). (C-D) Representative examples of implantation fields of diphtheria toxin–injected *CCR2*$^{+/RFP}$ single-transgenic mice (C) and *CCR2*$^{+/RFP}$;*CCR2-depleter*$^{+/0}$ bitransgenic littermates (D). Scale bars represent 10 μm.

the principal fibrinolytic protease and was recently shown to directly stimulate macrophage phagocytosis.[77] Therefore, we first implanted fibrin gels into plasminogen-deficient (*Plg*$^{-/-}$) and wild-type littermates and quantified fibrin uptake. Interestingly, although loss of plasminogen did not significantly affect the abundance of cells within the implantation zone (Figure 7A, examples in Figure 7D-E), it caused a dramatic reduction in the fraction of cells that internalized fibrin at 24 hours (Figure 7B, examples in Figure 7D-E), demonstrating a pivotal role of plasminogen in enabling the cellular uptake of extravascular fibrin. Consistent with this loss of cellular fibrin uptake, fluorescent fibrin gels implanted into plasminogen-deficient mice remained essentially intact when followed for up to 14 days, and gels implanted into plasminogen heterozygous-deficient (*Plg*$^{+/-}$) mice displayed reduced degradation when compared with littermate wild-type mice (Figure 7C). Even at 14 days after fibrin implantation, very few cells internalized fibrin in plasminogen-deficient mice (Figure 7F-G), showing that plasminogen deficiency likely is poorly compensated by alternative leukocyte fibrinolytic pathways[78] in the context of endocytic fibrin uptake.

To determine the role of plasminogen activators in endocytic fibrin uptake, we next implanted fibrin gels into uPA-deficient (*Plau*$^{-/-}$) mice, uPAR-deficient (*Plaur*$^{-/-}$) mice, and tPA-deficient (*Plat*$^{-/-}$) mice and their respective wild-type littermates. In contrast to the loss of plasminogen, individual loss of uPA or uPAR did not affect fibrin endocytosis, and loss of tPA caused only a small, nonsignificant reduction in endocytosis (Figure 7H-J).

The lack of effect of individual loss of uPA or tPA on fibrin endocytosis indicated that plasminogen activation was dispensable for plasminogen-dependent fibrin endocytosis, or, alternatively, that uPA and tPA activated plasminogen in a functionally redundant manner in this context. To discriminate between the 2 possibilities, we implanted fibrin gels into knockin mice homozygous for point mutations in the endogenous *Plg* gene that substitute the active site serine within the catalytic His-Ser-Asp triad of plasmin with alanine (*Plg*$^{S743A/S743A}$ mice) and their wild-type littermates. *Plg*$^{S743A/S743A}$ mice express normal levels of the mutant plasminogen, which can undergo activation site cleavage but is enzymatically inactive.[79] Like wholesale loss of plasminogen, loss of plasmin enzymatic activity dramatically reduced fibrin endocytosis (Figure 7K), demonstrating that plasmin-mediated fibrin cleavage is a prerequisite for cellular fibrin uptake and lysosomal degradation in vivo. Additional evidence for overlapping functions of uPA and tPA in activating plasminogen in this process was revealed by the much lower number of fibrin-endocytosing cells in fibrin-implanted uPA and tPA double-deficient (*Plau*$^{-/-}$;*Plat*$^{-/-}$) mice, as compared with tPA single-deficient *Plat*$^{-/-}$ littermates (Figure 7L). Taken together, the above studies reveal a novel mechanistic coupling of extracellular and endocytic fibrin degradation pathways (Figure 7M).

Discussion

We used intravital microscopy to investigate how fibrin is removed from extravascular space and found that removal of fibrin deposited in the mouse dermis involves endocytic uptake and lysosomal routing of the fibrin. We proceeded to characterize this endocytic fibrin degradation pathway at the cellular and molecular level and elucidated the following characteristics:

a. Fibrin endocytosis is executed primarily by CCR2 single-positive and CCR2, CX3CR1 double-positive macrophages that are recruited or emerge in response to fibrin deposition. Minor contributions from CX3CR1-positive, CCR2-negative macrophages, neutrophils, and fibroblasts were also identified.
b. Fibrin endocytosis requires plasminogen and plasminogen activation, likely to fragment fibrin to make it amenable for endocytic uptake, to expose cellular binding sites on the partially digested fibrin, or to stimulate general phagocytic activity.[77]
c. uPA and tPA have redundant functions in the activation of plasminogen in the context of fibrin endocytosis.
d. Fibrin endocytosis can take place in the absence of the fibrin receptors αMβ2 and ICAM-1 the multiligand macrophage endocytosis

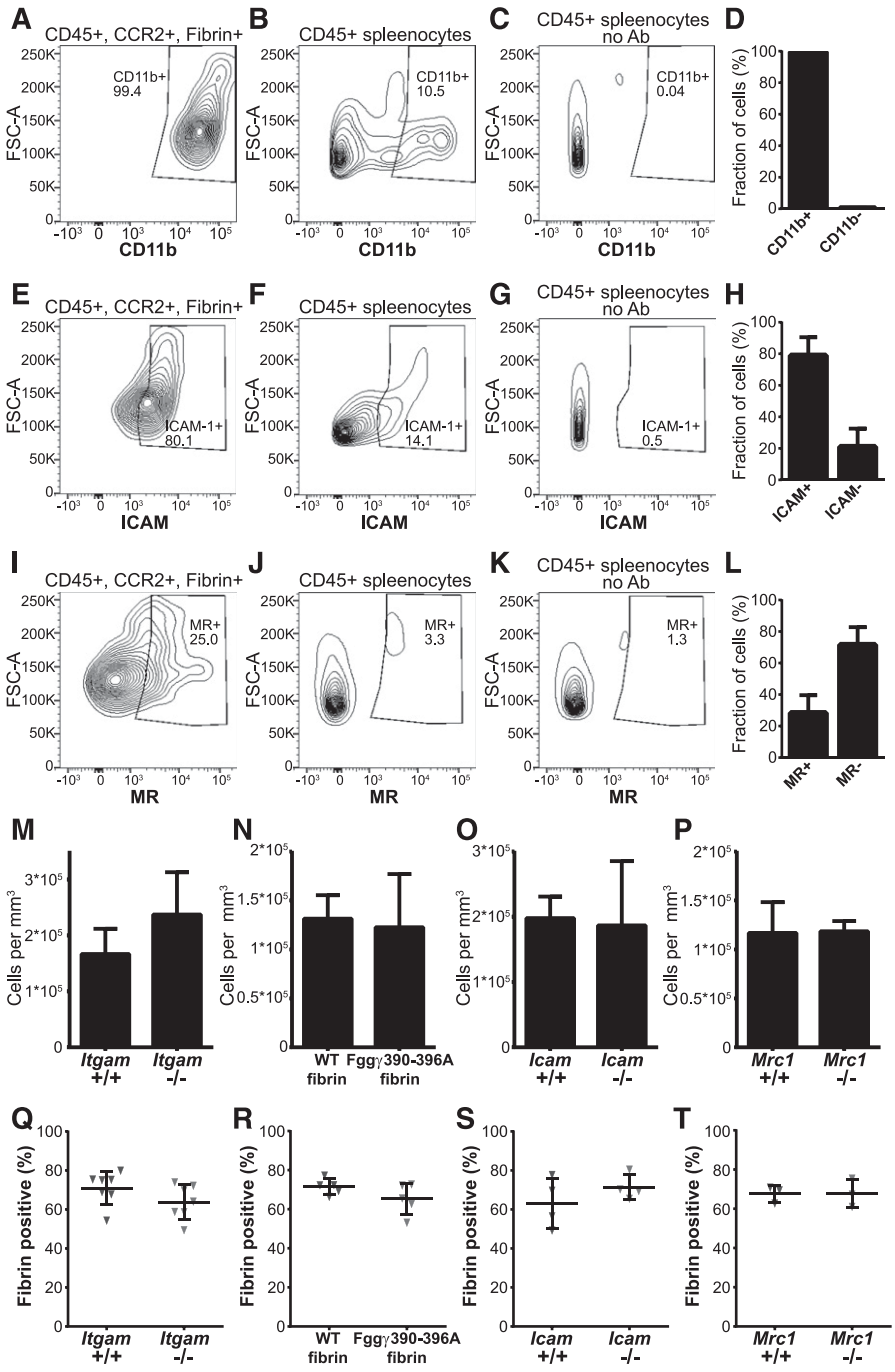

Figure 6. Effect of deletion of the candidate fibrin receptors αMβ2, ICAM-1, the principal myeloid integrin engagement site on fibrin, and the mannose receptor on endocytic fibrin uptake. (A-L) Expression of candidate fibrin-internalization receptors by CCR2-positive, fibrin-internalizing cells. (A,E,I) Representative examples of flow cytometry analysis of CD45-positive, CCR2-positive, fibrin-internalizing cells from fibrin-internalization zones stained with antibodies against CD11b (A), ICAM1 (E), and MR (I). (B,F,J) Representative examples of flow cytometry analysis of CD45-positive spleen cells stained with antibodies against CD11b (B), ICAM1 (F), and MR (J) as positive control. (C,G,K) Flow cytometry analysis of CD45-positive spleen cells with primary antibody omitted (negative control). Diagrams show intensity of staining vs forward scatter. Boxes show gate for positive signal with percentage of cell in gate indicated. (D,H,L) CD45-positive, CCR2-positive, fibrin-internalizing cells from fibrin internalization zones expressing CD11b (D, N = 3 mice), ICAM1 (H, N = 3 mice), and MR (L, N = 3 mice). Data are shown as mean with standard deviation. (M) Enumeration of cell accumulation in implantation zones from wild-type mice (left bars, N = 7 mice) and αMβ2-deficient *Itgam*$^{-/-}$ littermates (right bars, N = 6 mice). (N) Enumeration of cell accumulation in implantation zones from wild-type mice implanted with fibrin derived from wild-type mice (left bars, N = 5 mice) or with fibrin derived from *Fgg*$^{390\text{-}396A}$ littermates (right bars, N = 5 mice). (O) Enumeration of cell accumulation in implantation zones from wild-type mice (left bars, N = 4 mice) and ICAM1-deficient *Icam*$^{-/-}$ littermates (right bars, N = 4 mice). (P) Enumeration of cell accumulation in implantation zones from wild-type mice (left bars, N = 3 mice) and MR-deficient *Mrc1*$^{-/-}$ littermates (right bars, N = 3 mice). Data in panels M-P are shown as mean values and standard deviations. Significance was determined by Student *t* test (2 tailed). (Q) Enumeration of the fibrin-endocytosing fraction of cells in implantation zones from wild-type mice (left triangles) and αMβ2-deficient *Itgam*$^{-/-}$ littermates (right triangles). (R) Enumeration of the fibrin-endocytosing fraction of cells in implantation zones from wild-type mice implanted with fibrin derived from wild-type mice (left triangles) or with fibrin derived from *Fgg*$^{390\text{-}396A}$ littermates (right triangles). (S) Enumeration of the fibrin-endocytosing fraction of cells in implantation zones from wild-type mice (left triangles) and ICAM1-deficient *Icam*$^{-/-}$ littermates (right triangles). (T) Enumeration of the fibrin-endocytosing fraction of cells in implantation zones from wild-type mice (left triangles) and MR-deficient *Mrc1*$^{-/-}$ littermates (right triangles). Data in panels Q-T are shown as individual values for each mouse, as well as mean values and standard deviations. Significance was determined by Student *t* test (2 tailed).

receptor MR, and the principal myeloid integrin engagement site on fibrin.

The aggressive cellular uptake and lysosomal targeting of extravascular fibrin observed here at first glance is surprising, in light of the well-established pathways for extracellular plasminogen activation in the context of fibrinolysis. Our findings, however, support the emerging notion that extracellular and intracellular matrix degradation pathways are functionally linked in a sequential process orchestrated by specialized cells through the coordinated expression of specific cell-surface–located matrix-degrading enzymes and extracellular matrix receptors.[80-82] In this scenario, a limited number of proteolytic enzymes, endowed with the capacity to act on nondenatured cross-linked matrices (eg, plasmin and collagenase-type matrix metalloproteinases), execute the initial fragmentation of extracellular matrices, whereas bulk degradation takes place in the lysosome following the uptake of large extracellular matrix fragments.

The identification of macrophages as the principal cell type mediating intracellular fibrin degradation is not unexpected in light of the well-established role of macrophages as professional phagocytes and their high-level expression of plasminogen activators and receptors for plasmin(ogen) and plasminogen activator.[83-85] Importantly, however, the population of macrophages engaged in endocytic fibrin turnover in the dermis is different from the population of macrophages engaged in endocytic collagen turnover in the same tissue. Thus, whereas CCR2-positive inflammatory macrophages are primarily engaged in fibrin endocytosis, interstitial collagen is predominantly degraded through

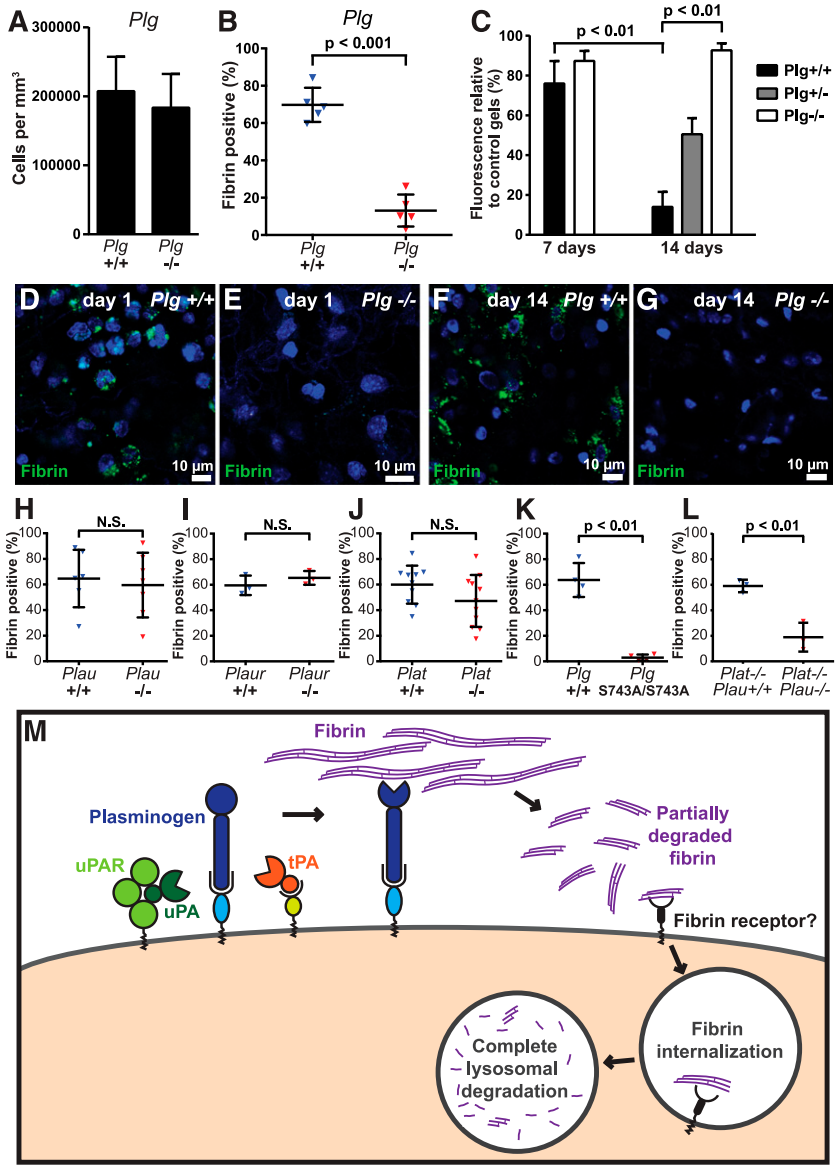

Figure 7. Plasminogen and plasmin activity is critical for endocytic fibrin degradation. (A) Loss of plasminogen does not affect cell recruitment to fibrin implantation zones. Total cell numbers in implantation zones from wild-type mice (left bar, N = 5 mice) and $Plg^{-/-}$ littermates (right bar, N = 5 mice). Data are shown as mean values with standard deviations. (B-G) Reduced fibrin endocytosis in plasminogen-deficient mice. (B) Enumeration of the fibrin endocytosing fraction of cells in implantation zones from wild-type mice (blue triangles) and $Plg^{-/-}$ littermates (red triangles). Data are shown as individual values for each mouse, as well as mean values and standard deviations. Significance was determined by Student *t* test (2 tailed). (C) Loss of plasminogen prevents extravascular fibrin degradation. Fluorescent fibrin gels were placed in subcutaneous space of $Plg^{+/+}$ (black bars, N = 3), $Plg^{+/-}$ (gray bar, N = 4), and $Plg^{-/-}$ (white bars, N = 3 [day 7] and N = 6 [day 14]) mice. The gels were extracted at 7 and 14 days after implantation, and fluorescence was measured. Data are expressed as percent residual fluorescence compared with control gels stored for the identical time period in the dark at 37°C in PBS with sodium azide. Significance was determined by 2-way ANOVA (comparison of days) and 1-way ANOVA (comparison of genotypes). (D-G) Representative examples of implantation zone from wild-type ($Plg^{+/+}$) (D,F) and littermate plasminogen-deficient ($Plg^{-/-}$) (E,G) mice 24 hours (D-E) and 14 days (F-G) after fibrin implantation. Multiple cells with endocytosed fibrin (green) are found in wild-type mice, but not in plasminogen-deficient mice, at both time points. (H-J) Individual deficiencies in uPA, uPAR, and tPA do not diminish endocytic fibrin uptake. Enumeration of fraction of cells in implantation zones from wild-type mice (blue triangles) and $Plau^{-/-}$ littermates (red triangles) (F), wild-type mice (blue triangles) and $Plaur^{-/-}$ littermates (red triangles) (G), and wild-type mice (blue triangles) and $Plat^{-/-}$ littermates (red triangles) (H). Data are shown as individual values for each mouse, as well as mean values and standard deviations. Significance was determined by Student *t* test (2 tailed). (K) Plasmin enzymatic activity is required for fibrin endocytosis. Enumeration of fraction of cells in implantation zones from wild-type mice (blue triangles) and $Plg^{S743A/S743A}$ littermates (red triangles). Data are shown as individual values for each mouse, as well as mean values and standard deviations. Significance was determined by Student *t* test (2 tailed). (L) Functional overlap of uPA and tPA in mediating fibrin endocytosis. Enumeration of fraction of cells in implantation zones from $Plat^{-/-}$ mice (blue triangles) and $Plat^{-/-}$;$Plau^{-/-}$ littermates (red triangles). Data are shown as individual values for each mouse, as well as mean values and standard deviations. Significance was determined by Student *t* test (2 tailed). (M) Hypothesized mechanism of extravascular fibrin clearance by inflammatory CCR2 macrophages. Cell-surface receptor-bound plasminogen on macrophages recruited to fibrin deposits is activated by cell-surface receptor-bound uPA and tPA. The resulting cell-surface–bound plasmin, protected from inactivation by α2-antiplasmin, partially degrades fibrin. The partially degraded fibrin is endocytosed by the CCR2-macrophages, possibly through an unidentified fibrin receptor different from αMβ2 and ICAM-1. Additional partially degraded fibrin may be made available for endocytosis by non–cell-surface–dependent plasminogen activation pathways (not shown). Fibrin-containing endocytic vesicles deliver their cargo to lysosomes, resulting in complete degradation of fibrin by lysomal proteases. N.S., not significant.

endocytosis by CCR2-negative macrophages with a noninflammatory, tissue-remodeling M2-polarization (this study and Madsen et al[62]). Macrophages display plasticity in terms of polarization,[86] and it remains to be established if this different phenotype of fibrin- and collagen-degrading macrophages is induced in response to the engagement of the 2 matrices, or if fibrin and collagen deposition attracts/retains

fundamentally different macrophage subpopulations. Whichever is the case, this finding makes excellent sense from a wound-healing perspective. Fibrin is the first matrix to be deposited in response to tissue injury, and, as the healing process progresses, this provisional fibrin matrix is replaced by a collagenous scar. The capacity of fibrin to attract or induce inflammatory macrophages capable of orchestrating a robust antibacterial response may be critical to the initial phase of the healing process, and the ability of collagen to attract noninflammatory M2-polarized wound-healing macrophages may be essential for scar resolution.

An unexpected finding in this study was the capacity of fibrin internalization to take place in the absence of the principal fibrin-binding myeloid cell integrin αMβ2 or the integrity of the principal integrin-binding site on fibrin. Although the former could be explained by compensation by other myeloid cell β2 integrins, removal of the integrin-binding RLSIGE motif on the fibrin γ chain completely abrogates macrophage adhesion to fibrin ex vivo.[3] The fibrin endocytosis pathway identified here thus appears to be fundamentally different from a previously described endocytosis pathway for soluble fibrin on cultured U-937 monocytoid cells,[58] which was described as being plasmin independent but dependent of αMβ2-mediated fibrin binding. An early study, in which endocytosis of soluble fibrin monomer by cultured peritoneal rabbit macrophages was followed by electron microscopy, provided evidence for a specific fibrin endocytosis receptor binding the N terminus of the α chain.[57] The proposition of a specific interaction with the α chain was based on the ability of a Gly-Pro-Arg peptide, mimicking the N terminus of the α chain, to block fibrin monomer endocytosis. However, we were unable to observe an effect of this peptide on the endocytosis of radiolabeled fibrin by cultured J774A.1 macrophage-like cells (unpublished data). Furthermore, overall fibrin uptake by these cells was very low, and the absence of an in vitro assay to mechanistically dissect the novel fibrin endocytotic pathway is a significant limitation of our study.

The redundancy of uPA and tPA in mediating plasminogen activation required for cellular uptake and lysosomal degradation of fibrin is well aligned with the observed fibrin-associated phenotypes of mice with single and combined plasminogen activator deficiency. Thus, deficiency in either uPA or tPA causes modest or no extravascular fibrin deposition and only small wound-healing defects, whereas combined uPA and tPA deficiency causes extensive extravascular fibrin deposition and severely compromised wound healing.[51,53] It is also consistent with the robust expression of receptors for both uPA and tPA on macrophages.[85,87] It should be noted, however, that our study does not exclude that alternative plasminogen activator–independent fibrinolytic pathways[78,88] contribute to endocytic fibrin uptake.

In summary, by using intravital microscopy, we have identified an intracellular fibrin degradation pathway that is engaged in extravascular fibrinolysis and is mechanistically distinct from previously described fibrinolytic pathways and from other extracellular matrix–degrading pathways.

Acknowledgments

The authors thank Dr Katerina Akassoglou for discussions stimulating the initiation of this work and Dr Eric G. Pamer for providing transgenic mice. We thank Drs Silvio Gutkind and Mary Jo Danton for critically reviewing this manuscript.

This research was supported by the Intramural Research Program of the National Institutes of Health, National Institute of Dental and Craniofacial Research, by the National Heart, Lung, and Blood Institute (R01 HL55374) and National Institute of Neurological Disorders and Stroke (R01 NS079639) (D.A.L.), National Heart, Lung, and Blood Institute (HL013423) (F.J.C.), and National Institute of Arthritis and Musculoskeletal and Skin Diseases (R01 AR056990) (M.J.F.). H.J.J. was supported by a Fellowship from the Danish Cancer Society.

Authorship

Contribution: M.P.M, D.H.M., H.J.J., D.E.S., R.S., K.H., and R.W. designed and performed the research; D.A.L. and F.J.C. bred and provided transgenic mice; M.J.F. purified and provided mutant mouse fibrinogen; T.H.B. and D.H.M. designed research, analyzed data, and wrote the paper.

Conflict-of-interest disclosure: The authors declare no competing financial interests.

Correspondence: Thomas H. Bugge, National Institute of Dental and Craniofacial Research, National Institutes of Health, 30 Convent Dr, Room 320, Bethesda, MD 20892; e-mail: thomas.bugge@nih.gov.

References

1. Doolittle RF. Fibrinogen and fibrin. *Annu Rev Biochem.* 1984;53:195-229.
2. Drew AF, Liu H, Davidson JM, Daugherty CC, Degen JL. Wound-healing defects in mice lacking fibrinogen. *Blood.* 2001;97(12):3691-3698.
3. Flick MJ, Du X, Witte DP, et al. Leukocyte engagement of fibrin(ogen) via the integrin receptor alphaMbeta2/Mac-1 is critical for host inflammatory response in vivo. *J Clin Invest.* 2004; 113(11):1596-1606.
4. Plow EF, Haas TA, Zhang L, Loftus J, Smith JW. Ligand binding to integrins. *J Biol Chem.* 2000; 275(29):21785-21788.
5. Forsyth CB, Solovjov DA, Ugarova TP, Plow EF. Integrin alpha(M)beta(2)-mediated cell migration to fibrinogen and its recognition peptides. *J Exp Med.* 2001;193(10):1123-1133.
6. Drew AF, Kaufman AH, Kombrinck KW, et al. Ligneous conjunctivitis in plasminogen-deficient mice. *Blood.* 1998;91(5):1616-1624.
7. Schott D, Dempfle CE, Beck P, et al. Therapy with a purified plasminogen concentrate in an infant with ligneous conjunctivitis and homozygous plasminogen deficiency. *N Engl J Med.* 1998; 339(23):1679-1686.
8. Hidayat AA, Riddle PJ. Ligneous conjunctivitis. A clinicopathologic study of 17 cases. *Ophthalmology.* 1987;94(8):949-959.
9. Tefs K, Gueorguieva M, Klammt J, et al. Molecular and clinical spectrum of type I plasminogen deficiency: A series of 50 patients. *Blood.* 2006; 108(9):3021-3026.
10. Schuster V, Mingers AM, Seidenspinner S, Nüssgens Z, Pukrop T, Kreth HW. Homozygous mutations in the plasminogen gene of two unrelated girls with ligneous conjunctivitis. *Blood.* 1997;90(3):958-966.
11. Pantanowitz L, Bauer K, Tefs K, et al. Ligneous (pseudomembranous) inflammation involving the female genital tract associated with type-1 plasminogen deficiency. *Int J Gynecol Pathol.* 2004;23(3):292-295.
12. Ciftçi E, Ince E, Akar N, Dogru U, Tefs K, Schuster V. Ligneous conjunctivitis, hydrocephalus, hydrocele, and pulmonary involvement in a child with homozygous type I plasminogen deficiency. *Eur J Pediatr.* 2003; 162(7-8):462-465.
13. Baykul T, Bozkurt Y. Destructive membranous periodontal disease (ligneous periodontitis): a case report and 3 years follow-up. *Br Dent J.* 2004;197(8):467-468.
14. Watts P, Suresh P, Mezer E, et al. Effective treatment of ligneous conjunctivitis with topical plasminogen. *Am J Ophthalmol.* 2002;133(4): 451-455.
15. Bugge TH, Flick MJ, Daugherty CC, Degen JL. Plasminogen deficiency causes severe thrombosis but is compatible with development and reproduction. *Genes Dev.* 1995;9(7):794-807.

16. Bugge TH, Kombrinck KW, Flick MJ, Daugherty CC, Danton MJ, Degen JL. Loss of fibrinogen rescues mice from the pleiotropic effects of plasminogen deficiency. *Cell.* 1996;87(4): 709-719.

17. Ploplis VA, Carmeliet P, Vazirzadeh S, et al. Effects of disruption of the plasminogen gene on thrombosis, growth, and health in mice. *Circulation.* 1995;92(9):2585-2593.

18. de Giorgio-Miller A, Bottoms S, Laurent G, Carmeliet P, Herrick S. Fibrin-induced skin fibrosis in mice deficient in tissue plasminogen activator. *Am J Pathol.* 2005;167(3):721-732.

19. Drew AF, Tucker HL, Liu H, Witte DP, Degen JL, Tipping PG. Crescentic glomerulonephritis is diminished in fibrinogen-deficient mice. *Am J Physiol Renal Physiol.* 2001;281(6): F1157-F1163.

20. Sachs BD, Baillie GS, McCall JR, et al. p75 neurotrophin receptor regulates tissue fibrosis through inhibition of plasminogen activation via a PDE4/cAMP/PKA pathway. *J Cell Biol.* 2007; 177(6):1119-1132.

21. Schachtrup C, Lu P, Jones LL, et al. Fibrinogen inhibits neurite outgrowth via beta 3 integrin-mediated phosphorylation of the EGF receptor. *Proc Natl Acad Sci USA.* 2007;104(28): 11814-11819.

22. Akassoglou K, Adams RA, Bauer J, et al. Fibrin depletion decreases inflammation and delays the onset of demyelination in a tumor necrosis factor transgenic mouse model for multiple sclerosis. *Proc Natl Acad Sci USA.* 2004;101(17): 6698-6703.

23. Vidal B, Serrano AL, Tjwa M, et al. Fibrinogen drives dystrophic muscle fibrosis via a TGFbeta/ alternative macrophage activation pathway. *Genes Dev.* 2008;22(13):1747-1752.

24. Flick MJ, LaJeunesse CM, Talmage KE, et al. Fibrin(ogen) exacerbates inflammatory joint disease through a mechanism linked to the integrin alphaMbeta2 binding motif. *J Clin Invest.* 2007;117(11):3224-3235.

25. Danø K, Andreasen PA, Grøndahl-Hansen J, Kristensen P, Nielsen LS, Skriver L. Plasminogen activators, tissue degradation, and cancer. *Adv Cancer Res.* 1985;44:139-266.

26. Collen D, Lijnen HR. The fibrinolytic system in man. *Crit Rev Oncol Hematol.* 1986;4(3):249-301.

27. Thorsen S. The mechanism of plasminogen activation and the variability of the fibrin effector during tissue-type plasminogen activator-mediated fibrinolysis. *Ann N Y Acad Sci.* 1992; 667:52-63.

28. Hoylaerts M, Rijken DC, Lijnen HR, Collen D. Kinetics of the activation of plasminogen by human tissue plasminogen activator. Role of fibrin. *J Biol Chem.* 1982;257(6):2912-2919.

29. Collen D. On the regulation and control of fibrinolysis. Edward Kowalski Memorial Lecture. *Thromb Haemost.* 1980;43(2):77-89.

30. Collen D, Lijnen HR. Thrombolytic agents. *Thromb Haemost.* 2005;93(4):627-630.

31. Plow EF, Freaney DE, Plescia J, Miles LA. The plasminogen system and cell surfaces: evidence for plasminogen and urokinase receptors on the same cell type. *J Cell Biol.* 1986;103(6 Pt 1): 2411-2420.

32. Beebe DP, Miles LA, Plow EF. A linear amino acid sequence involved in the interaction of t-PA with its endothelial cell receptor. *Blood.* 1989;74(6): 2034-2037.

33. Felez J, Chanquia CJ, Levin EG, Miles LA, Plow EF. Binding of tissue plasminogen activator to human monocytes and monocytoid cells. *Blood.* 1991;78(9):2318-2327.

34. Hajjar KA, Harpel PC, Jaffe EA, Nachman RL. Binding of plasminogen to cultured human endothelial cells. *J Biol Chem.* 1986;261(25): 11656-11662.

35. Ling Q, Jacovina AT, Deora A, et al. Annexin II regulates fibrin homeostasis and neoangiogenesis in vivo. *J Clin Invest.* 2004; 113(1):38-48.

36. Hajjar KA, Jacovina AT, Chacko J. An endothelial cell receptor for plasminogen/tissue plasminogen activator. I. Identity with annexin II. *J Biol Chem.* 1994;269(33):21191-21197.

37. Hajjar KA, Hamel NM, Harpel PC, Nachman RL. Binding of tissue plasminogen activator to cultured human endothelial cells. *J Clin Invest.* 1987;80(6):1712-1719.

38. Miles LA, Parmer RJ. Plasminogen receptors: the first quarter century. *Semin Thromb Hemost.* 2013;39(4):329-337.

39. Connolly BM, Choi EY, Gårdsvoll H, et al. Selective abrogation of the uPA-uPAR interaction in vivo reveals a novel role in suppression of fibrin-associated inflammation. *Blood.* 2010; 116(9):1593-1603.

40. Ellis V, Scully MF, Kakkar VV. Plasminogen activation initiated by single-chain urokinase-type plasminogen activator. Potentiation by U937 monocytes. *J Biol Chem.* 1989;264(4):2185-2188.

41. Stephens RW, Pöllänen J, Tapiovaara H, et al. Activation of pro-urokinase and plasminogen on human sarcoma cells: a proteolytic system with surface-bound reactants. *J Cell Biol.* 1989;108(5): 1987-1995.

42. Rønne E, Behrendt N, Ellis V, Ploug M, Danø K, Høyer-Hansen G. Cell-induced potentiation of the plasminogen activation system is abolished by a monoclonal antibody that recognizes the NH2-terminal domain of the urokinase receptor. *FEBS Lett.* 1991;288(1-2):233-236.

43. Ellis V, Danø K. Potentiation of plasminogen activation by an anti-urokinase monoclonal antibody due to ternary complex formation. A mechanistic model for receptor-mediated plasminogen activation. *J Biol Chem.* 1993; 268(7):4806-4813.

44. Ellis V, Behrendt N, Danø K. Plasminogen activation by receptor-bound urokinase. A kinetic study with both cell-associated and isolated receptor. *J Biol Chem.* 1991;266(19): 12752-12758.

45. Dewerchin M, Nuffelen AV, Wallays G, et al. Generation and characterization of urokinase receptor-deficient mice. *J Clin Invest.* 1996;97(3): 870-878.

46. Deindl E, Ziegelhöffer T, Kanse SM, et al. Receptor-independent role of the urokinase-type plasminogen activator during arteriogenesis. *FASEB J.* 2003;17(9):1174-1176.

47. Kitching AR, Holdsworth SR, Ploplis VA, et al. Plasminogen and plasminogen activators protect against renal injury in crescentic glomerulonephritis. *J Exp Med.* 1997;185(5): 963-968.

48. Carmeliet P, Moons L, Dewerchin M, et al. Receptor-independent role of urokinase-type plasminogen activator in pericellular plasmin and matrix metalloproteinase proteolysis during vascular wound healing in mice. *J Cell Biol.* 1998; 140(1):233-245.

49. Shanmukhappa K, Sabla GE, Degen JL, Bezerra JA. Urokinase-type plasminogen activator supports liver repair independent of its cellular receptor. *BMC Gastroenterol.* 2006;6:40.

50. Bezerra JA, Currier AR, Melin-Aldana H, et al. Plasminogen activators direct reorganization of the liver lobule after acute injury. *Am J Pathol.* 2001;158(3):921-929.

51. Bugge TH, Flick MJ, Danton MJ, et al. Urokinase-type plasminogen activator is effective in fibrin clearance in the absence of its receptor or tissue-type plasminogen activator. *Proc Natl Acad Sci USA.* 1996;93(12):5899-5904.

52. Bugge TH, Suh TT, Flick MJ, et al. The receptor for urokinase-type plasminogen activator is not essential for mouse development or fertility. *J Biol Chem.* 1995;270(28):16886-16894.

53. Carmeliet P, Schoonjans L, Kieckens L, et al. Physiological consequences of loss of plasminogen activator gene function in mice. *Nature.* 1994;368(6470):419-424.

54. Longstaff C, Merton RE, Fabregas P, Felez J. Characterization of cell-associated plasminogen activation catalyzed by urokinase-type plasminogen activator, but independent of urokinase receptor (uPAR, CD87). *Blood.* 1999; 93(11):3839-3846.

55. Walker JB, Nesheim ME. The molecular weights, mass distribution, chain composition, and structure of soluble fibrin degradation products released from a fibrin clot perfused with plasmin. *J Biol Chem.* 1999;274(8):5201-5212.

56. Ryu JK, Petersen MA, Murray SG, et al. Blood coagulation protein fibrinogen promotes autoimmunity and demyelination via chemokine release and antigen presentation. *Nat Commun.* 2015;6:8164.

57. Gonda SR, Shainoff JR. Adsorptive endocytosis of fibrin monomer by macrophages: evidence of a receptor for the amino terminus of the fibrin alpha chain. *Proc Natl Acad Sci USA.* 1982;79(15): 4565-4569.

58. Simon DI, Ezratty AM, Francis SA, Rennke H, Loscalzo J. Fibrin(ogen) is internalized and degraded by activated human monocytoid cells via Mac-1 (CD11b/CD18): a nonplasmin fibrinolytic pathway. *Blood.* 1993;82(8): 2414-2422.

59. Andersen RB, Elling P. Immunofluorescent demonstration of intracellular fibrin in synovial tissue. *Ann Rheum Dis.* 1972;31(1):59-64.

60. Ghadially FN, Roy S. Ultrastructure of synovial membrane in rheumatoid arthritis. *Ann Rheum Dis.* 1967;26(5):426-443.

61. Riddle JM, Bluhm GB, Barnhart MI. Interrelationships between fibrin, neutrophils and rheumatoid synovitis. *J Reticuloendothel Soc.* 1965;2(5):420-436.

62. Madsen DH, Leonard D, Masedunskas A, et al. M2-like macrophages are responsible for collagen degradation through a mannose receptor-mediated pathway. *J Cell Biol.* 2013;202(6): 951-966.

63. Panchuk-Voloshina N, Haugland RP, Bishop-Stewart J, et al. Alexa dyes, a series of new fluorescent dyes that yield exceptionally bright, photostable conjugates. *J Histochem Cytochem.* 1999;47(9):1179-1188.

64. Sandoval RM, Kennedy MD, Low PS, Molitoris BA. Uptake and trafficking of fluorescent conjugates of folic acid in intact kidney determined using intravital two-photon microscopy. *Am J Physiol Cell Physiol.* 2004;287(2):C517-C526.

65. Masedunskas A, Weigert R. Intravital two-photon microscopy for studying the uptake and trafficking of fluorescently conjugated molecules in live rodents. *Traffic.* 2008;9(10):1801-1810.

66. Muzumdar MD, Tasic B, Miyamichi K, Li L, Luo L. A global double-fluorescent Cre reporter mouse. *Genesis.* 2007;45(9):593-605.

67. Krempen K, Grotkopp D, Hall K, et al. Far upstream regulatory elements enhance position-independent and uterus-specific expression of the murine alpha1(I) collagen promoter in transgenic mice. *Gene Expr.* 1999;8(3):151-163.

68. Geissmann F, Jung S, Littman DR. Blood monocytes consist of two principal subsets with distinct migratory properties. *Immunity.* 2003; 19(1):71-82.

69. Hohl TM, Rivera A, Lipuma L, et al. Inflammatory monocytes facilitate adaptive CD4 T cell responses during respiratory fungal infection. *Cell Host Microbe.* 2009;6(5):470-481.

70. Ugarova TP, Lishko VK, Podolnikova NP, et al. Sequence gamma 377-395(P2), but not gamma 190-202(P1), is the binding site for the alpha MI-domain of integrin alpha M beta 2 in the gamma C-domain of fibrinogen. *Biochemistry.* 2003; 42(31):9365-9373.

71. Ugarova TP, Solovjov DA, Zhang L, et al. Identification of a novel recognition sequence for integrin alphaM beta2 within the gamma-chain of fibrinogen. *J Biol Chem.* 1998;273(35): 22519-22527.

72. Languino LR, Plescia J, Duperray A, et al. Fibrinogen mediates leukocyte adhesion to vascular endothelium through an ICAM-1-dependent pathway. *Cell.* 1993;73(7):1423-1434.

73. Martinez-Pomares L, Wienke D, Stillion R, et al. Carbohydrate-independent recognition of collagens by the macrophage mannose receptor. *Eur J Immunol.* 2006;36(5):1074-1082.

74. Madsen DH, Ingvarsen S, Jürgensen HJ, et al. The non-phagocytic route of collagen uptake: a distinct degradation pathway. *J Biol Chem.* 2011; 286(30):26996-27010.

75. Jürgensen HJ, Johansson K, Madsen DH, et al. Complex determinants in specific members of the mannose receptor family govern collagen endocytosis. *J Biol Chem.* 2014;289(11): 7935-7947.

76. Malovic I, Sørensen KK, Elvevold KH, et al. The mannose receptor on murine liver sinusoidal endothelial cells is the main denatured collagen clearance receptor. *Hepatology.* 2007;45(6): 1454-1461.

77. Das R, Ganapathy S, Settle M, Plow EF. Plasminogen promotes macrophage phagocytosis in mice. *Blood.* 2014;124(5):679-688.

78. Plow EF. Leukocyte elastase release during blood coagulation. A potential mechanism for activation of the alternative fibrinolytic pathway. *J Clin Invest.* 1982;69(3):564-572.

79. Iwaki T, Malinverno C, Smith D, et al. The generation and characterization of mice expressing a plasmin-inactivating active site mutation. *J Thromb Haemost.* 2010;8(10): 2341-2344.

80. Lee H, Overall CM, McCulloch CA, Sodek J. A critical role for MT1-MMP in collagen phagocytosis. *Mol Biol Cell.* 2006;17(11): 4812-4826.

81. Madsen DH, Bugge TH. Imaging collagen degradation in vivo highlights a key role for M2-polarized macrophages in extracellular matrix degradation. *OncoImmunology.* 2013;2(12): e27127.

82. Madsen DH, Engelholm LH, Ingvarsen S, et al. Extracellular collagenases and the endocytic receptor, urokinase plasminogen activator receptor-associated protein/Endo180, cooperate in fibroblast-mediated collagen degradation. *J Biol Chem.* 2007;282(37):27037-27045.

83. Andronicos NM, Chen EI, Baik N, et al. Proteomics-based discovery of a novel, structurally unique, and developmentally regulated plasminogen receptor, Plg-RKT, a major regulator of cell surface plasminogen activation. *Blood.* 2010;115(7):1319-1330.

84. Felez J, Miles LA, Plescia J, Plow EF. Regulation of plasminogen receptor expression on human monocytes and monocytoid cell lines. *J Cell Biol.* 1990;111(4):1673-1683.

85. Brownstein C, Deora AB, Jacovina AT, et al. Annexin II mediates plasminogen-dependent matrix invasion by human monocytes: enhanced expression by macrophages. *Blood.* 2004;103(1): 317-324.

86. Mosser DM, Edwards JP. Exploring the full spectrum of macrophage activation. *Nat Rev Immunol.* 2008;8(12):958-969.

87. Plesner T, Ralfkiaer E, Wittrup M, et al. Expression of the receptor for urokinase-type plasminogen activator in normal and neoplastic blood cells and hematopoietic tissue. *Am J Clin Pathol.* 1994;102(6):835-841.

88. Lund LR, Green KA, Stoop AA, et al. Plasminogen activation independent of uPA and tPA maintains wound healing in gene-deficient mice. *EMBO J.* 2006;25(12):2686-2697.